

Programming a Raytracer Using Python

Maike Lenz

Abstract—In this project, a raytracing program was designed using Python. The optical raytracer manages to simulate raybundles of a given diameter and propagate them through various optical elements. Specifically, this project focused on spherical refracting surfaces. The program can find intercepts of the surface and a given ray, and propagate said ray through the surface by using Snell's Law. In order to test the program, both orientations of a plano-convex lens were compared by determining the amount of spherical aberration in each case. The program can also find the paraxial focal point of a singular spherical refracting surface and place the output plane there. This value is very close to the theoretical prediction of the paraxial focal point according to the paraxial approximation.

I. INTRODUCTION

LENSES are used in a broad range of contexts from telescopes to bundling lasers to cut materials. In order to calibrate them effectively, computational raytracers are commonly used to calculate the optimum focal point of the lens. This is especially useful for instances where a laser needs to be positioned at the correct distance from a lens to illuminate a surface with maximum intensity. In this project, Python was used to code a program which finds the paraxial focal point of an optical environment. Object oriented programming enabled the involved rays, refracting surfaces, and output planes to interact with each other as objects. The project simulates either a single light ray or a beam of rays, which are refracted by an optical element, such as a lens, and then hit an output plane. Crucial components of the code included being able to determine intercepts of the rays with a spherical surface component or a plane, to refract light rays by Snell's Law, to determine the paraxial focal point of the optical component, and to plot the ray diagrams. In order to focus a beam of light effectively, it is important to minimise spherical aberration. A measure of how focused a ray bundle is was calculated in the form of the rms value of the deviation from the z -axis of each ray's intercept with the output plane.

II. BACKGROUND

A. Snell's Law

Snell's law describes the angles through which a ray is refracted when it crosses a boundary between two materials with refractive indices n_1 and n_2 . It is typically given as [1]

$$n_1 \sin(\theta_1) = n_2 \sin(\theta_2) \quad (1)$$

where θ_1 is the angle of incidence and θ_2 is the angle of refraction of the ray with the normal of the refracting surface. In this project, it was more useful to consider the vector form [2] of the equation, which is

$$\mathbf{k}_2 = \frac{n_1}{n_2} \mathbf{k}_1 + \left(\frac{n_1}{n_2} \cos(\theta_1) - \cos(\theta_2) \right) \mathbf{n} \quad (2)$$

where k_1 is the incident vector, k_2 is the refracted vector, and n is the surface normal pointing from the light source to the surface. All vectors are unit vectors.

B. Spherical Aberration

1) *Spherical Refracting Surfaces*: Spherically refracting surfaces were a crucial part of this investigation. This kind of surface can be thought of as the slice of a sphere up until the aperture radius, r_a . The z -axis is defined as passing through the centre of the sphere from left to right, with z_0 being the intercept of the surface with the axis, and o being the position of the centre of curvature, as illustrated in Fig.1. Spherically refracting surfaces are characterised by their curvature, which is the reciprocal of the curvature radius, r_c . Simply put, positive curvature means the left side of the sphere, whereas negative curvature is the right side. A schematic of a spherically refractive surface is shown in Fig.1.

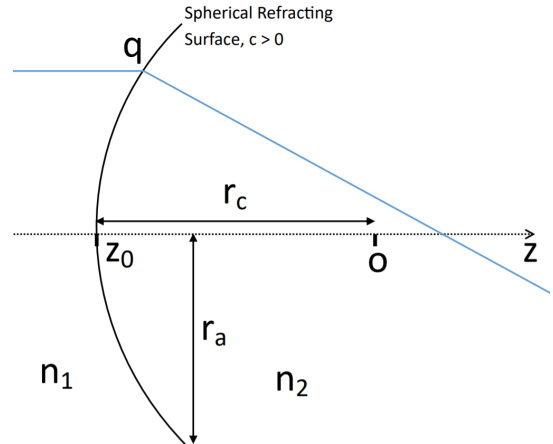


Fig. 1: Schematic diagram of a spherical refracting surface between materials with refractive indices n_1 and n_2 where r_c is the radius of curvature, r_a is the aperture radius, q is the intercept with a ray, o is the centre of curvature, and z_0 is the intercept between the surface and the z -axis.

Whenever a flat refracting surface was used in this project, it was defined as a spherical refracting surface with curvature equal to zero.

2) *Spherical Aberration*: Rays which start at different distances from the z -axis and travel parallel to it, are refracted by different angles when they pass through a spherical refracting surface. Spherical aberration means that rays further away from the axis (shown in blue in Fig.2.) intercept the z -axis before paraxial rays do. Paraxial rays intercept the surface closer to the axis (red in Fig.2.). When the focal point of a refracting surface is determined, the paraxial focal point is normally considered; this is the point at which paraxial rays

intercept the z - axis. This is point b in Fig.2. However, the outer rays have continued propagating beyond the z - axis by the time the focal point is reached, which means that the beam of rays hits the paraxial plane at b in a circle of a given radius rather than a point. This is referred to as longitudinal spherical aberration [3] , or LSA.

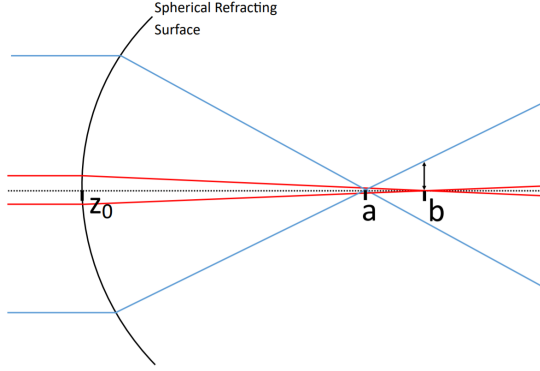


Fig. 2: Simple ray diagram demonstrating spherical aberration. Rays which intercept a refracting surface further away from the z - axis (blue), intercept said axis at any point a , which is before the paraxial focal point, b .

A very focused beam of rays means that the LSA is small. In this project, an output plane was located at the paraxial focal point. The root mean square value of the distance between each individual ray's intercept with the plane and the z -axis was found as a measure of how sharp the produced image would be. This was calculated using the equation

$$\text{rms} = \sqrt{\frac{\sum_{i=1}^N x_i^2 + y_i^2}{N}} \quad (3)$$

where x_i and y_i are the x - y coordinates of an individual ray's intercept with the output plane, and N is the number of rays in the beam.

C. Paraxial Focal Point

Throughout the investigation, a method to determine the paraxial focal point of a lens using a test-ray was developed. However, this value needed to be compared to the theoretical prediction. For this, the paraxial approximation was used. Any given spherical refracting surface has a focusing power, which determines the amount by which light is refracted through it. The focal power is given by [4]

$$P = \frac{n_2 - n_1}{r_c} \quad (4)$$

where n_1 and n_2 are the refractive indices before and beyond the surface respectively, and r_c is the radius of curvature of the spherical surface. The focal distance is the reciprocal of the focal power [5]. Hence, the z - coordinate of the paraxial focal point is given by

$$f = \frac{r_c}{n_2 - n_1} + z_0 + r_c \quad \text{for } n_2 > n_1 \quad (5)$$

$$f = \frac{r_c}{n_2 - n_1} + z_0 \quad \text{for } n_2 < n_1 \quad (6)$$

since r_c is technically negative for a surface with negative curvature.

These equations are an approximation assuming that the angles of incidence and refraction are very small, hence why they apply to paraxial rays only.

III. METHODOLOGY

A. Setting up the Classes

The main three classes that make up the code are Ray, RayBundle, and OpticalElement. The two classes SphericalRefraction and OutputPlane both inherit from OpticalElement. Their methods include finding intercepts with rays, refracting rays, and plotting them. They are related as illustrated in Fig.3.

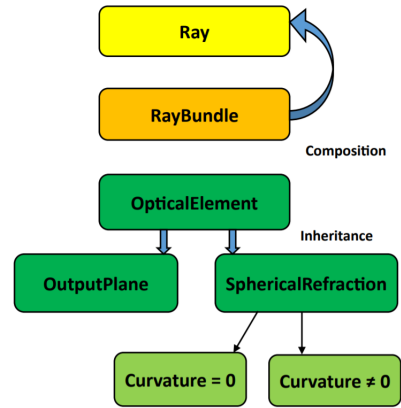


Fig. 3: Block Diagram to show the relationship between the classes of objects involved in the project.

Ray represents any given ray of light characterised by a list of all position and direction vectors. RayBundle has a method generate() to configure a raybundle of a given radius consisting of concentric circles of rays with uniform density. The RayBundle class is therefore composed of objects of the Ray class. The rays are distributed in the x - y plane as shown in Fig.4.

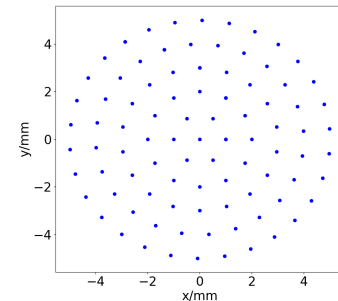


Fig. 4: Scatter graph to show the start points of the rays in a raybundle of diameter 10 mm in the x - y plane.

This raybundle can then be propagated through the optical system. Propagating the ray means that each surface in turn finds the intercept of the ray with itself, and refracts the ray by applying Snell's Law. This continues throughout all the surfaces until the output plane is reached and the rays terminate.

B. Finding Intercepts

1) *Flat Surfaces*: The incident ray has a know starting point and direction. For a refracting surface with zero curvature, the z - coordinate of the intercept is fixed at z_0 . Hence, simple vector calculations can be used to find the scalar distance between the last point of the ray and the intercept, l :

$$l = \frac{z_0 - p_z}{k_z} \quad (7)$$

where p_z and k_z are the z - components of the position and the direction vector of the ray respectively. Now the intercept q is

$$q = p + lk \quad (8)$$

The same method was used to determine the intercept of any given ray with the output plane.

2) *Curved Surfaces*: For a curved surface, the distance between the last point of the ray and the intercept, l , is given by [6]

$$l = -\mathbf{r} \cdot \hat{\mathbf{k}} \pm \sqrt{(\mathbf{r} \cdot \hat{\mathbf{k}})^2 - (|\mathbf{r}|^2 - r_c^2)} \quad (9)$$

where \mathbf{r} is the vector from the centre of curvature of the spherical surface to the last point of the ray, $\hat{\mathbf{k}}$ is the last direction vector of the ray, and r_c is the radius of curvature. For positive curvatures, the square root was subtracted from the dot product to find the leftmost intercept. For negative curvatures, the square root was added.

C. Determining the Paraxial Focal Point

In order to find the paraxial focal point of the surface, a test-ray close to the axis was configured and propagated through each surface in turn. Finally, the point at which it intercepts the z - axis was found and the output plane was positioned there. The test-ray started at coordinates $p = [0.1, 0, 0]$ and travelled in the direction $k = [0, 0, 1]$. A smaller starting x - coordinate would have increased the accuracy of the focal point; however, rounding errors meant that smaller values returned None. Fig.5. shows a ray diagram of a raybundle with diameter 60 mm being refracted by a spherical surface at $z_0 = 100\text{mm}$ with curvature 0.03 mm^{-1} . The refractive index beyond the surface is 1.5168. The output plane is located at the paraxial focal point.

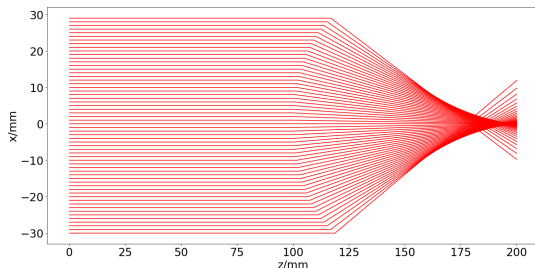


Fig. 5: Ray diagram demonstrating LSA at the focal point.

Towards the right side of Fig.5., LSA is clearly shown, as the rays which started furthest from the z - axis spread out.

The theoretical prediction for the z - coordinate of the paraxial focal point was calculated with equation (5) to give

$$f_{theory} = 200.0\text{mm}$$

whereas the value found using the test-ray method was

$$f_{test} = 200.0\text{mm}$$

Both values are the same, so the test-ray method works for this case. The deviation from the theoretical value is negligible. Testing of the code confirmed this for all tested scenarios.

IV. TESTING BOTH ORIENTATIONS OF A PLANO-CONVEX LENS

A plano-convex lens consists of one flat and one convex side. These were generated by two spherical refracting surfaces, one with curvature 0.03mm^{-1} and one with 0mm^{-1} . The correct orientation of this type of lens means that light passes through the curved surface first and then the flat surface, as shown in Fig.6. With the wrong orientation, the light beam hits the planar surface, and then the curved surface, as in Fig.7. The spherical surface has a curvature of -0.03mm^{-1} in this case because it is pointing to the right. The LSA of the plano-convex lens in both of these cases were compared for a beam consisting of concentric circles of light rays with a diameter of 10 mm. The refractive index of the inside of the lens was taken to be 1.5168. Again, the output plane was positioned to be at the paraxial focal point, which was found by using the test-ray method as outlined previously.

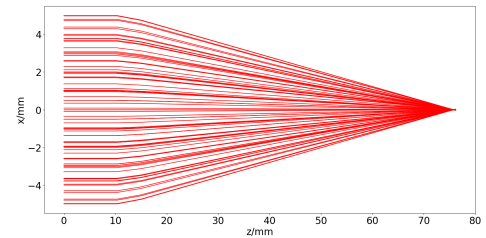


Fig. 6: Ray diagram of the cross section at $y = 0$ of a raybundle of diameter 10 mm being refracted by a plano-convex lens orientated the correct way (curved surface, then flat surface)

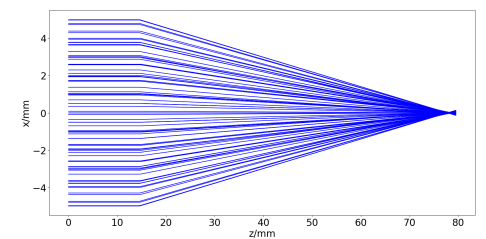


Fig. 7: Ray diagram of the cross section at $y = 0$ of a raybundle of diameter 10 mm being refracted by a plano-convex lens orientated the wrong way (flat surface, then curved surface)

There are significant differences between the two cases. As seen faintly in the ray diagrams, when the lens is correctly

orientated, the rays are refracted twice rather than only changing direction once. This is because a ray travelling along the normal of a planar refracting surface does not change direction as it is propagated through it. If the ray has already been refracted through the convex surface, it travels at an angle to the normal of the plane and will be refracted again.

Not only is the focal point closer to z_0 when the lens faces the correct way, but spherical aberration has a visibly smaller effect. This was investigated further by plotting a scatter diagram of the rays hitting the output plane at the paraxial focal point for both cases, as illustrated in Fig.8.

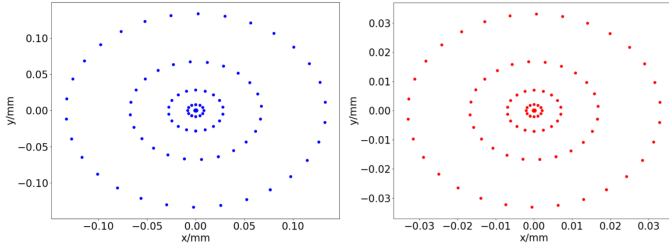


Fig. 8: Scatter graphs of the rays intercepting the output plane at the paraxial focal point. The wrong lens orientation is in blue on the left, the correct one in red on the right.

Both of these diagrams have the expected shape, where the outer concentric circles hit the surface further away from the z - axis and were refracted by a much greater angle. The radius of the outer circle is much smaller in the red graph in Fig.8., when the lens is orientated correctly. The rms values of the distance from the z - axis gave the following results

correct orientation: rms = 0.0209mm

wrong orientation: rms = 0.0843mm

As expected, the rms value of the spherical aberration of the plano-convex lens as it is orientated the correct way around is much smaller. This is because the beam is more focused. Orientating a plano convex lens is crucial, since it quarters the LSA.

V. EVALUATION

The main source of error in this investigation comes from rounding and small angle approximations. For example, the test-ray to find the paraxial focal point could be placed closer to the z - axis. This would increase the accuracy of the paraxial focal point. However, any smaller x - value was rounded down by Python to give zero. This did not yield a useful result.

The project assumed that the effects of diffraction of the light rays due to the surfaces were negligible. The scale of diffraction is approximately [6]

$$\text{diffraction scale} = \frac{\lambda f}{D} \quad (10)$$

where λ is the wavelength of light, f is the focal distance, and D is the beam diameter. Assuming a wavelength of 588 nm [6], the diffraction scale for a 10 mm diameter beam incident to a spherical refracting surface of curvature 0.03 mm^{-1} is about 4×10^{-6} mm. This value is very much smaller than

the amount of spherical aberration, which is approximately of the order of magnitude 10^{-1} mm. The effect of diffraction is therefore negligible.

A main part of the investigation was Snell's Law, which predicts the angle at which a ray will be refracted. Rays may not behave exactly as predicted by Snell's Law [7] when it is applied locally at a given point, i.e. the intercept of the ray and the refracting surface. However, since the aim of the project is more macroscopic and aimed to find the focal point of a collection of rays rather than accurately modelling a single ray at every point, this possible small deviation can be ignored.

Although testing of the code was carried out after every step, it is possible that there are certain scenarios which cause errors in the or let systematic errors arise. However, for simple cases, the code works as predicted.

VI. CONCLUSION

In this project, a raytracer program was successfully designed. It manages to simulate various optical systems consisting of rays, spherical refracting surfaces, planar surfaces, and output planes. The numerical comparisons of the paraxial focal points and the amounts of spherical aberration with theoretical prediction showed that there are no significant systematic errors. It must be considered that the theoretical formulae used to test the accuracy of the simulation are themselves small angle approximations, so ideally this program should be tested experimentally as well.

As an extension, other shapes of refracting surfaces could be incorporated into the program. In order to minimise LSA, it may be best to use an aspherical surface, or other types of lenses; e.g. a biconvex lens. This would have been the next step in the investigation, given more time. This program provides a good starting point for further testing. Any other optical elements can be added and use the OpticalElement class as a base class.

REFERENCES

- [1] A. K. Ghatak and K. Thyagarajan, *Contemporary optics*. Plenum Press, 1978.
- [2] A. S. Glassner, *An Introduction to ray tracing*. Academic Press, 1989.
- [3] T. T. Smith, "Spherical aberration in thin lenses," *Scientific Papers of the Bureau of Standards*, vol. 18, pp. 559–584, 1922.
- [4] F. G. Smith and J. H. Thomson, *Optics*. John Wiley Sons, 1995.
- [5] H. J. Pain, *The physics of vibrations and waves*. Wiley, 1993.
- [6] R. Kingham, *Project A: An Optical Ray Tracer*. Imperial College London, 2018.
- [7] W. Guo, "Formulation of light focusing through a plano-convex spherical lens in wave optics," *Journal of the Optical Society of America A*, vol. 28, no. 7, p. 1496, 2011.